

## EUROPEAN LABORATORY FOR PARTICLE PHYSICS

CERN-EP/98-164  
9 October 1998**TWO-DIMENSIONAL READOUT OF GEM DETECTORS**A. Bressan, R. De Oliveira, A. Gandi, J.-C. Labbé, L. Ropelewski and F. Sauli  
(CERN, Geneva, Switzerland)D. Mörmann, T. Müller, H.J. Simonis  
(Inst. Exp. Kernphysik, Karlsruhe, Germany)

## ABSTRACT

The recently introduced Gas Electron Multiplier (GEM) permits the amplification of electrons released by ionizing radiation in a gas by factors approaching ten thousand; larger gains can be obtained combining two GEMs in cascade. We describe methods for implementing two- and three-dimensional projective localization of radiation, with sub-millimeter accuracy, making use of specially manufactured and patterned pick-up electrodes. Easy to implement and flexible in the choice of the readout geometry, the technology has the distinctive advantage of allowing all pick-up electrodes to be kept at ground potential, thus substantially improving the system simplicity and reliability. Preliminary results demonstrating the two-dimensional imaging capability of the devices are provided and discussed, as well as future perspectives of development.

Submitted to Nucl. Instrum. Meth. in Phys. Res.

*Corresponding author: [fabio.sauli@cern.ch](mailto:fabio.sauli@cern.ch)*



## 1. INTRODUCTION

Recently introduced [1], the Gas Electron Multiplier has been extensively studied in order to improve the operating performances and fully exploit its potentialities [2-11]. In the simplest configuration (Fig. 1) a GEM detector consists of a drift electrode, a conversion and drift region, a GEM mesh collecting and multiplying the charge in a gas avalanche, and an induction gap in which a high electric field is used to extract and drift the electrons towards the collecting electrodes (a patterned printed circuit board). Thanks to the large effective gains achievable (up to  $10^4$ ), full efficiency of detection and very good localization accuracies have been demonstrated for minimum ionizing particles, releasing in a thin gap few tens of primary ion pairs; cascading two GEM meshes, larger gains and better performances can be achieved [4, 10].

In all measurements described so far, the pick-up electrode consisted of a simple printed circuit board with parallel strips at a small pitch (typically 200  $\mu\text{m}$ ). Although the electric field is set rather high in the induction gap, to efficiently collect electrons generated by the avalanche process within the GEM channels, its value (5 to 10 kV/cm) is low enough to effectively block the propagation of accidental discharges to the readout electrode. This is a substantial advantage, as compared to alternative devices, for the survivability of the delicate readout electronics. Since only electrons are collected and detected, the signal has a fast rise time without slow tails as those induced by the motion of positive ions in other micro-pattern devices. Capable of withstanding very high fluxes, well above  $10^5$  Hz/mm<sup>2</sup> [10], the device appears suitable for high rate, large area imaging in various applied fields.

## 2. TWO-DIMENSIONAL READ-OUT ELECTRODES GEOMETRY

We have extended the GEM detector principle to include several types of projective two-dimensional readouts; this is done using as pick-up electrode a specially manufactured double-level thin polymer foil, with pads or strips interconnected in various patterns. In the electron collection mode, a basic feature of the design, both read-out electrodes can be kept at ground potential.

The method of manufacturing the pick-up electrodes is a direct extension of the one developed for the GEM meshes. Two sets of parallel metal strips are engraved, using conventional printed circuit technology on the two sides of a thin polymer (kapton) foil. After gluing the foil on a thin insulating support, the polymer in the interstices between the upper strips is removed with a solvent, enabling the bottom layer to collect part of the electron charge. Both the support plate and the adhesive have of course to safely endure the entire process. Fig. 2a and b show schematically the geometry of a cartesian and a small stereo angle projective readout board, respectively; the pictures in Fig. 3 and 4 show close views of the two corresponding patterns successfully manufactured and tested. For practical reasons (availability of high-density readout electronics), we have used a

pitch of 200  $\mu\text{m}$  for all read-out strips, although the results of measurements suggest that, with a typical cluster size of around 400  $\mu\text{m}$  fwhm, a wider pitch would provide similar performances with larger signals on each strip, at the cost of a slightly reduced two-track separation [11]. The patterns have around 500 individual strips on each side, covering the full active area of the GEM detector (10x10  $\text{cm}^2$ ) and have been successfully made on 25  $\mu\text{m}$  and 50  $\mu\text{m}$  thick polymer foils, the thin one being preferable for better sharing of the charge and reduction of material.

With proper choice of the geometry, the average collected charge in the two projections can be made approximately equal. The geometrical signal sharing (ratio of collection areas seen by the charge) for the pattern in Fig. 2a is given by  $s_1 p_2 / (s_2 p_1 - s_1 s_2)$ , where  $s_1$ ,  $s_2$  and  $p_1$ ,  $p_2$  are the top and bottom strip widths and pitch, respectively. For the pattern of Fig. 2b the pick-up surfaces are identical; the stereo angle between the two projective coordinates is given by  $\tan(L/p)$ . Because of the finite thickness of the insulating support, however, the fraction of the electron signal on the top layer is actually larger than computed by geometry; for 25 and 50  $\mu\text{m}$  foils, we have measured a difference by a factor between 2 and 5, that can be corrected adjusting the geometry or, as described later, by the application of a moderate (few tens of volts) polarization voltage between the two layers.

### 3. EXPERIMENTAL SET-UP

All measurements described here have been made with a detector consisting of a single GEM, a drift space and a readout board as illustrated in Fig. 1; as filling gas, we have used a mixture of argon and carbon dioxide in the volume proportions 70-30. Although in all detectors the full active area of 10x10  $\text{cm}^2$  was powered, only smaller sets of strips were readout in each projection due to the limited number of electronics channels available. As radiation source, we have used a collimated 5.9 keV  $^{55}\text{Fe}$  X-ray source, or an X-ray generator with copper anti-cathode and the main line at 8 keV.

Several circuits were used for the readout: a fast amplifier-shaper based on the PreShape chip, with  $\sim 40$  ns shaping times [12], a multiple amplifier-shaper developed at CERN [13], or a multi-channel commercial charge amplifier<sup>1</sup>. The results depend little on the amplifier used, in view of the fact that in the GEM detector only the (fast) electron component of the charge is detected on the induction electrode (no ion tail cancellation or ballistic deficit corrections are present); for high rate applications, however, only the faster circuits should be used.

Exposing the detector to the X-ray source, we have recorded event per event the induced charge profiles on sets of adjacent strips with gated analogue-to digital converters. The trigger for gating the ADC was provided by the global signal picked up through a HV capacitor from the lower GEM electrode, facing the strips; for local studies, a linear fan-out inserted on one or more channels permitted to trigger on selected regions. Data were analyzed on-line to deduce pulse height spectra, correlation and cluster size on the two projections.

---

<sup>1</sup> Charge pre-amplifier Mod. A422 made by CAEN SPA, Viareggio (Italy).

Although the described readout concept allows for both coordinates to be kept at ground potentials, to compensate for an initial non optimal choice of geometry (an equal width of the strips), we have enhanced the collection efficiency of the lower electrode applying to it a moderate positive potential (few tens of volts to the grounded upper electrode). This is simply allowed by the polarization input available on one of the amplifiers cards. The range of signal sharing adjustment that could be achieved as a function of offset voltage between the readout patterns is shown in Fig. 5; at a value around 70 V, the effective gains as seen by the two equal width pick-up electrodes balance. While this voltage difference is considerably lower than any dangerous value for safe operation, an adjustment of the geometry (distance and area of the strips) that permits to obtain equal sharing of the charge between the two coordinates, kept both at ground, is obviously preferable and has been adopted in the improved layouts used for most of the measurements.

#### 4. EXPERIMENTAL RESULTS

Using the cartesian readout board shown in Fig. 3, we have recorded the charge profile on perpendicular sets of 16 strips, irradiating the detector with a well collimated  $^{55}\text{Fe}$  source. For each event, we compute the integrated charge over threshold (cluster charge) in the two projections. Fig. 6 shows the correlation plot between the total cluster charge recorded on the two projections; the scales have been normalized to the X-ray energy spectrum, having the main line at 5.9 keV and the argon escape around 3.2 keV. The projections on the two axis are given in Figs. 7a and b, while Fig. 7c corresponds to a projection along a line at  $45^\circ$ . The width of the inclined projection represents the resolution power of the correlation; for the main line, it corresponds to around 17% fwhm. The correlation is rather good, particularly taking into account the various intrinsic sources of dispersion, such as electronics noise and non collected channel-to-channel gain variations, only roughly corrected in this phase of the analysis.

Exposing the detector to a uniform radiation source (a wide beam from an X-ray tube) through a thin copper foil mask with open slits of various widths we have obtained the 2-D image shown in Fig. 7; the full size of the pattern is  $8.5 \times 7.5 \text{ mm}^2$ , with slits varying in width from one mm to  $200 \mu\text{m}$ . The fast signal picked up from the GEM electrode facing the read-out board was used to generate the trigger and ADC gate. The thickness of the mask,  $200 \mu\text{m}$ , is not sufficient to absorb all the radiation (8 keV), thus producing a uniform background at a level around 10% as seen in the figure. A projection of pairs of parallel patterns along the direction of the slits is shown in Figs. 9a and 9b; from the slope of the edges one can deduce a resolution of around  $100 \mu\text{m}$  from 10 to 90% that includes the (unknown) divergence of the beam and the non negligible range of the photoelectrons produced by the 8 keV line (5 keV for the majority of conversions in argon). Further studies are on the way to estimate the resolution of the method for contrasted objects.

## 5. SUMMARY AND FURTHER DEVELOPMENTS

The large proportional gains achievable with GEM devices (single or double) permit the detection and localization, on suitably patterned pick-up electrodes, of ionization released by fast particles or soft X-rays in a gas conversion volume. A special technology, based on the one developed for the GEM electrodes themselves, permit to manufacture pick-up electrodes with two-dimensional projective read-out. With a proper design of the geometry, and using a thin etched polymer foil to separate the two layers, the signal can be almost equally shared between the electrodes, both operated at ground potential. Preserving a good energy resolution in the two projections ( $\sim 18\%$  fwhm at 6 keV), the method should permit to associate pairs of coordinates in multi-track events resolving the ambiguities arising from the use of projective read-out; further studies of the resolution power and localization accuracy for minimum ionizing particles are in preparation. The detector offers a self-gating function, making use of the fast overall signal detected on the GEM electrode facing the read-out board; this is an essential feature for detection of neutral radiation.

In order to obtain a better uniformity of response, we are also considering alternative pick-up electrode designs, requiring the use of metal-plated holes but having the advantage of a coplanar and more uniform readout. Two possible schemes are shown in Fig. 10a and b. On the left, peanut-shaped induction pads are interconnected on the back side to form perpendicular strips; in Fig. 10b hexagonal pads are interconnected on the back side along three directions at  $60^\circ$  to each other, providing ambiguity-free multi-hit capability. This would be particularly interesting for example in the field of Cherenkov ring imaging, where patterns with several tens of points (single electron avalanches) are produced.

In both proposed schemes, and in view of the requirements on the pads size for good position accuracy (a mm or less), a refined technology for making plated-through holes on the thin kapton foils is required, an evolution of the one developed for GEMs, and has been already successfully tested at CERN.

The ultimate patterning is of course the read-out of individual pads, requiring the use of high density electronics such as the one developed for silicon devices [14, 15]. As most of these circuits, developed for the needs of particle physics, require a trigger to operate, the possibility to obtain an energy or timing signal from the GEM electrodes permit their use for medical imaging.

## REFERENCES

- [1] F. Sauli, Nucl. Instrum. Methods **A386** (1997) 531.
- [2] R. Bouclier, M. Capeáns, W. Dominik, M. Hoch, J.-C. Labbé, G. Million, L. Ropelewski, F. Sauli, A. Sharma, IEEE Trans. Nucl. Sci. **NS-44** (1997) 646.
- [3] C. Büttner, M. Capeáns, W. Dominik, M. Hoch, J.C. Labbé, G. Manzin, G. Million, L. Ropelewski, F. Sauli, A. Sharma, Nucl. Instr. Methods **A409** (1998) 79.
- [4] J. Benlloch, A. Bressan, C. Büttner, M. Capeáns, M. Gruwé, M. Hoch, J.C. Labbé, A. Placci, L. Ropelewski, F. Sauli, A. Sharma, R. Veenhof, IEEE Trans. Nucl. Sci. **NS-45** (1998) 234.
- [5] J. Benlloch, A. Bressan, M. Capeáns, M. Gruwé, M. Hoch, J.C. Labbé, A. Placci, L. Ropelewski, F. Sauli, Further developments of the Gas Electron Multiplier (GEM), Wire Chamber Conference (Vienna, Feb. 22-26, 1998). CERN-EP/98-50. Subm. Nucl. Instrum. Methods (1998).
- [6] A. Bondar, A. Buzulutskov, F. Sauli, L. Shekhtman, High and low pressure operation of the Gas Electron Multiplier, Wire Chamber Conference (Vienna, Feb. 23-27, 1998). Subm. Nucl. Instrum. Methods (1998).
- [7] A. Bressan, A. Buzulutskov, L. Ropelewski, F. Sauli, L. Shekhtman, High gain operation of GEM in pure argon, Budker INP 98-59. Subm. Nucl. Instr. Methods (1998).
- [8] R. Chechik, A. Breskin, G. Garty, J. Mattout, F. Sauli, E. Shefer, First results on the GEM operated at low gas pressures, Wire Chamber Conference (Vienna, Feb. 23-27, 1998). WIS-98/08. Subm. Nucl. Instrum. Methods (1998).
- [9] W. Beaumont, T. Beckers, J. DeTroy, V. Van Dyck, O. Bouhali, F. Udo, C. VanderVelde, W. Van Doninck, P. Vanlaer, V. Zhukov, Studies of an MSGC equipped with a GEM grid as a tracking device, Wire Chamber Conference (Vienna, Feb. 23-27, 1998). Subm. Nucl. Instrum. Methods (1998).
- [10] A. Bressan, M. Hoch, P. Pagano, L. Ropelewski, F. Sauli, S. Biagi, A. Buzulutskov, M. Gruwé, A. Sharma, D. Moermann, G. De Lentdecker, High rate behavior and discharge limits in micro-pattern detectors, CERN-EP/98-139. Subm. Nucl. Instr. Methods (1998).
- [11] A. Bressan, J.C. Labbé, P. Pagano, L. Ropelewski, F. Sauli, Beam tests of the gas electron multiplier, Subm. Nucl. Instrum. Methods (1998).
- [12] J.F. Clergeau, D. Contardo, R. Haroutunian, G. Smadja, LYCEN/9424 (1994).
- [13] P. Jarron, F. Anghinolfi, E. Delagne, W. Dabrowski, L. Scharfetter, Nucl. Instr. Methods **A377** (1996) 435.
- [14] P. Weilhammer, E. Nygård, W. Dulinski, A. Czermak, F. Djama, S. Gadomski, S. Roe, A. Rudge, F. Shopper, J. Strobel, Nucl. Instr. Methods **A383** (1996) 89.
- [15] D.D. Bari and e. al, Nucl. Instr. Methods **A395** (1996) 391.

## FIGURE CAPTIONS

Fig. 1: Schematics of a single-GEM detector with double-sided printed circuit board read-out.

Fig. 3: Two possible projective pick-up patterns: cartesian (a) and small-angle (B). The fractional charge sharing between the two layers can be adjusted by proper choice of the geometry.

Fig. 3: Close view of the cartesian read-out pattern, manufactured on 25  $\mu\text{m}$  thick kapton with 5  $\mu\text{m}$  copper. The pitch is 200  $\mu\text{m}$  and the strip width 90 and 140  $\mu\text{m}$ , respectively.

Fig. 4: Close view of the small angle projective pattern. The pitch is 200  $\mu\text{m}$  and the metal strip width about 90  $\mu\text{m}$  in both planes.

Fig. 5: Effect on the charge sharing of the potential difference between the two layers (50  $\mu\text{m}$  apart). For this measurement, a cartesian pattern with equal strip width ( $\sim 50 \mu\text{m}$ ) was used.

Fig. 6: Two dimensional charge correlation plot for events produced by a collimated 5.9 keV X-ray source; the scales are given in keV equivalent units.

Fig. 6: Distribution of cluster charge in the X (bottom layer) coordinate, normalized to the energy scale.

Fig. 7: Distribution of cluster charge in the Y (top layer) coordinate.

Fig. 8: Two-dimensional image obtained with an absorber mask, irradiated with a parallel beam at 8 keV. The background ( $\sim 10\%$ ) is due to the residual transmission of the copper absorber, 200  $\mu\text{m}$  thick.

Fig. 9a: Selective projection along the Y axis of the two patterns with slits parallel to the coordinate.

Fig. 9b: Projection along the X axis of the two patterns with slits parallel to the coordinate.

Fig. 10: Alternative read-out patterns with coplanar pick-up electrodes.



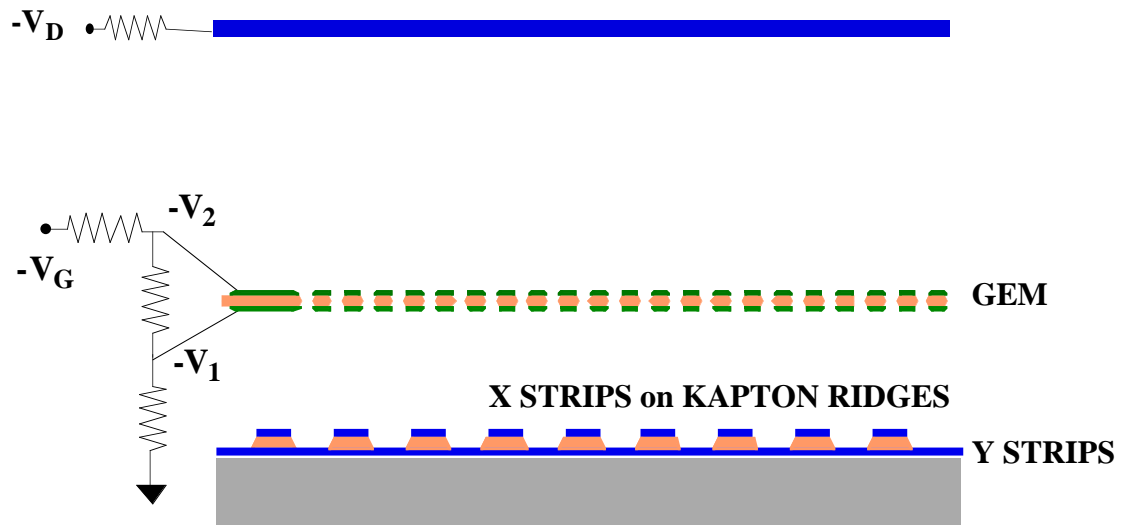


Fig 1

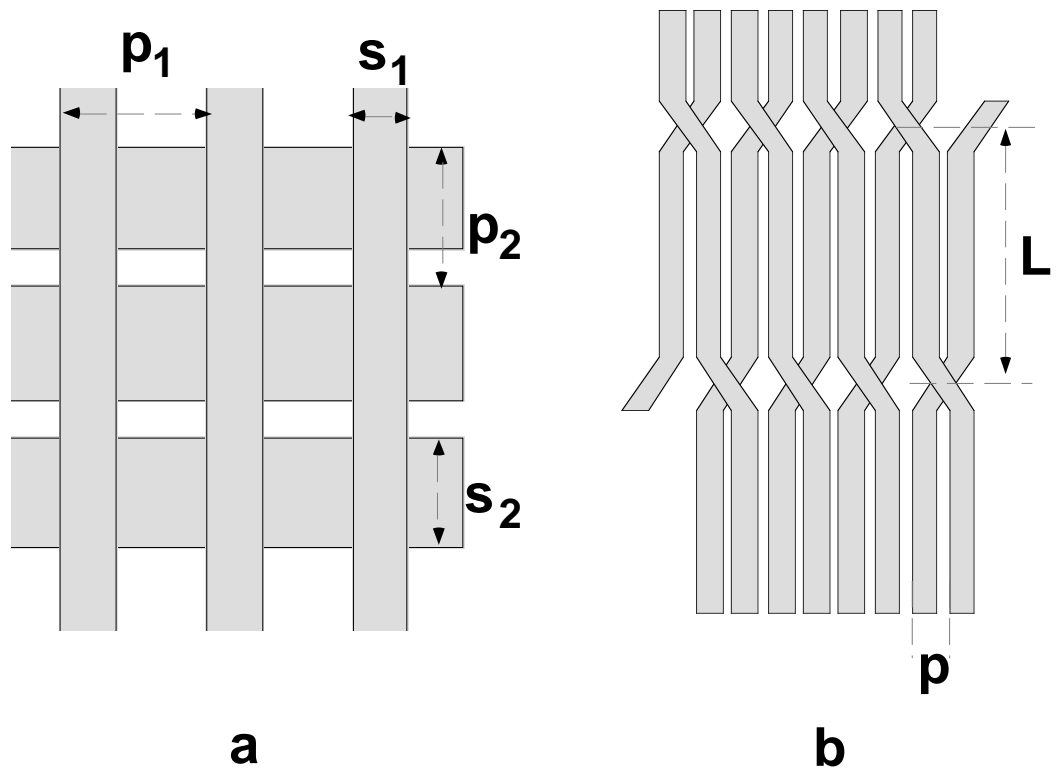


Fig. 2

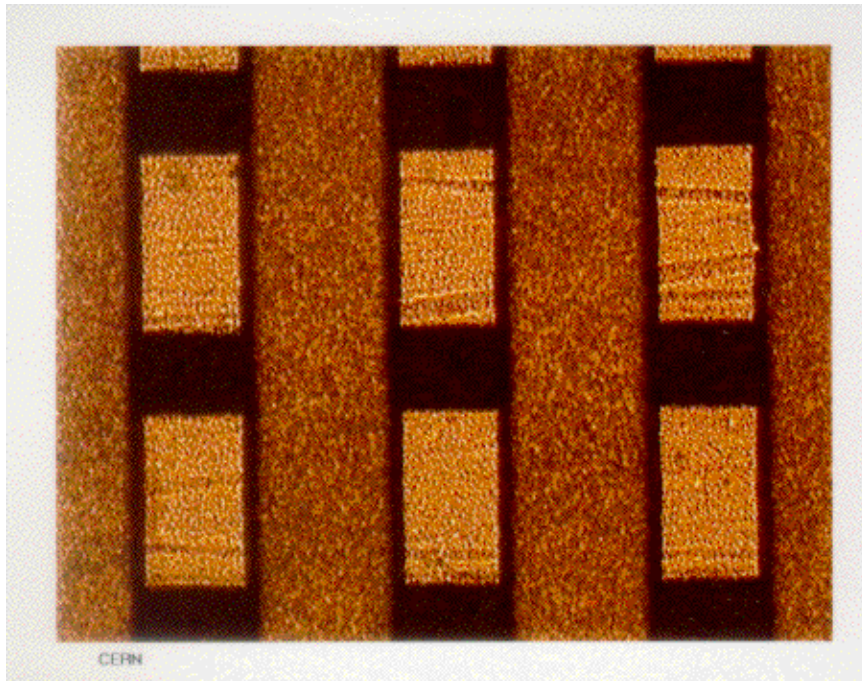


Fig. 3

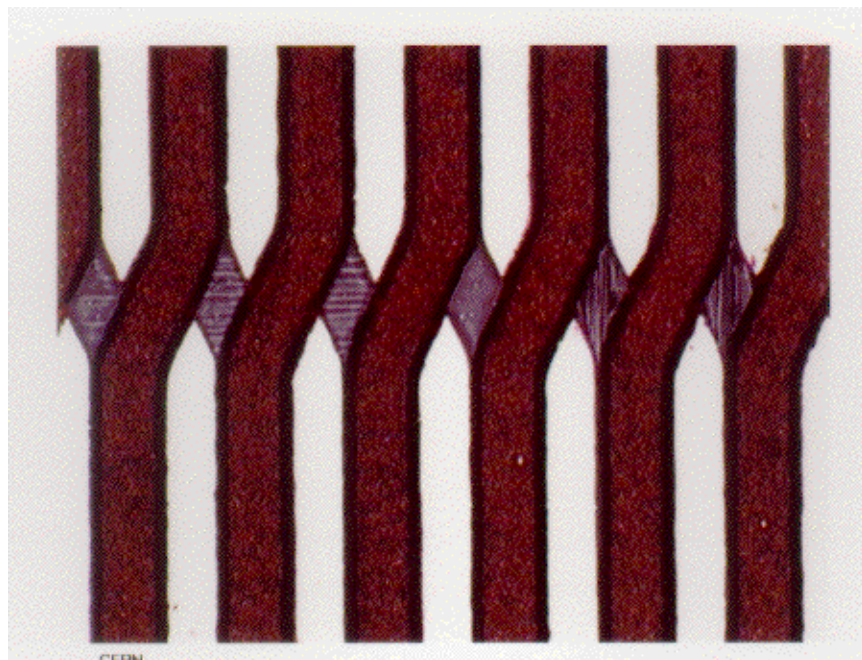


Fig. 4

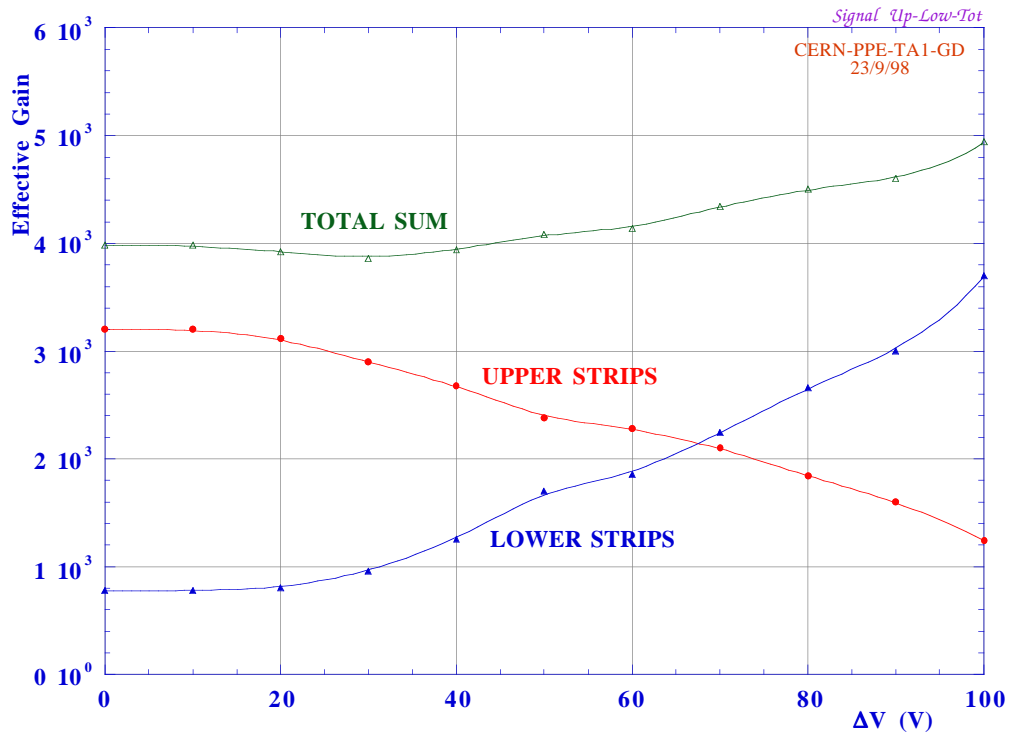


Fig. 5

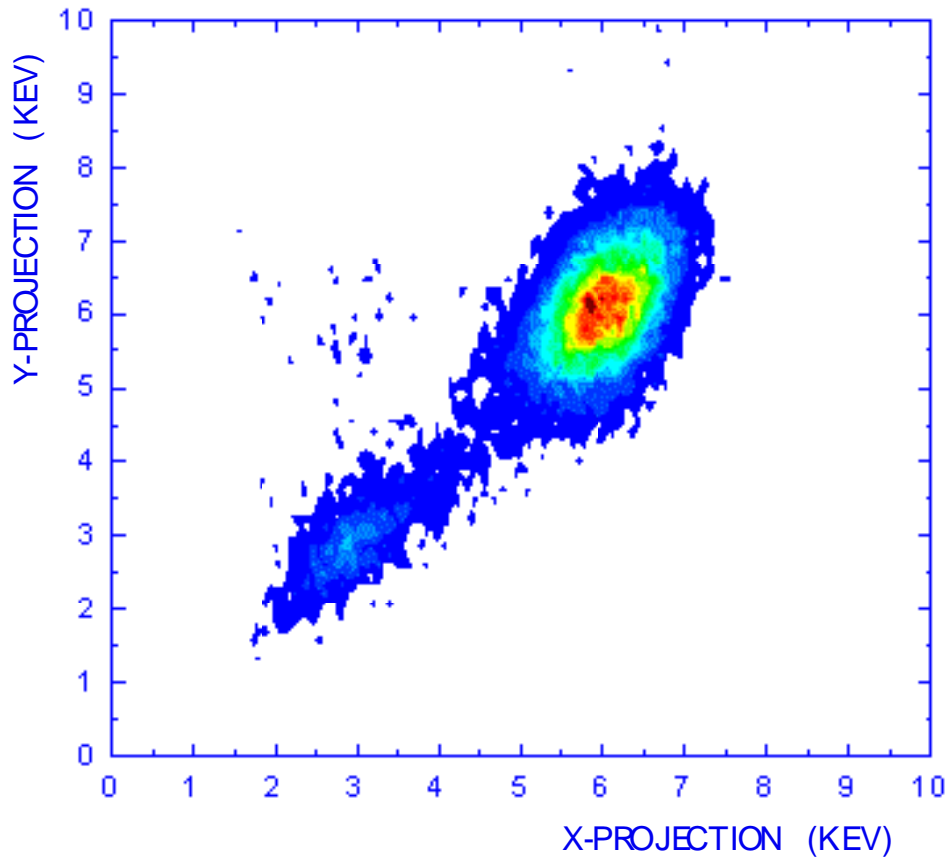
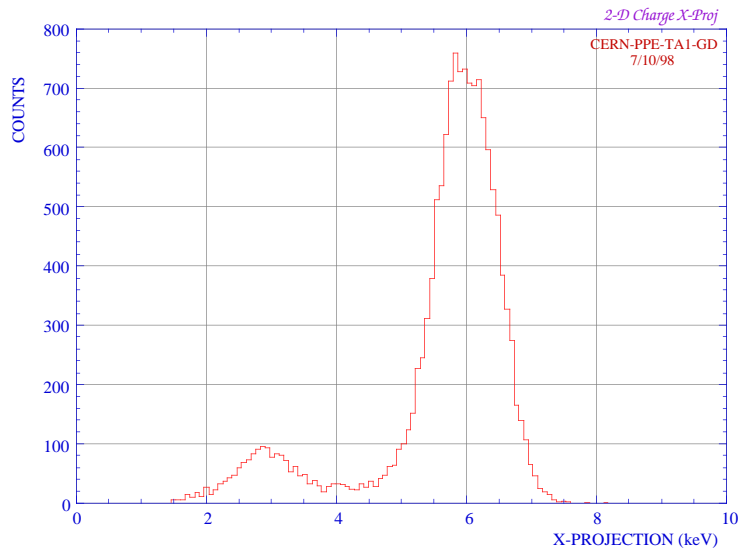
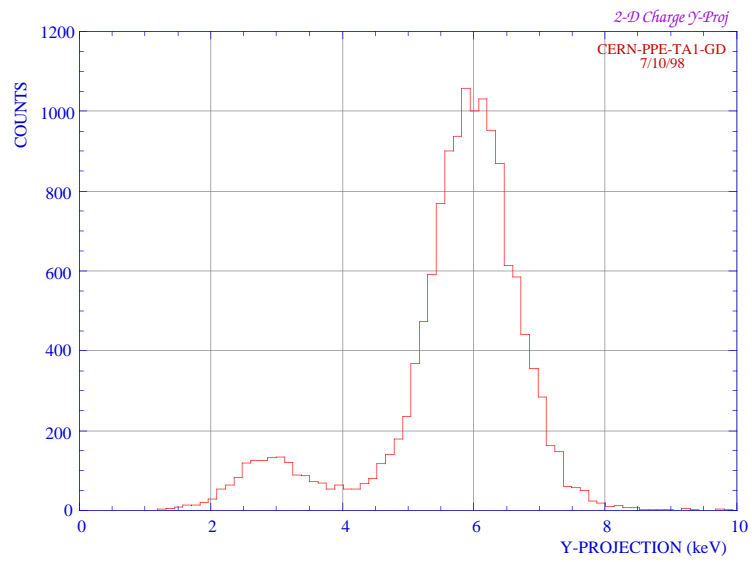


Fig. 6



**Fig. 7a**



**Fig. 7b**

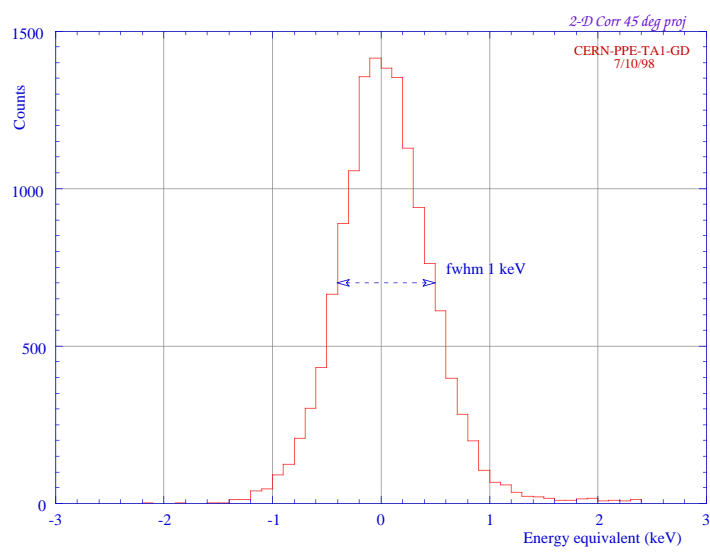


**Fig. 7c**

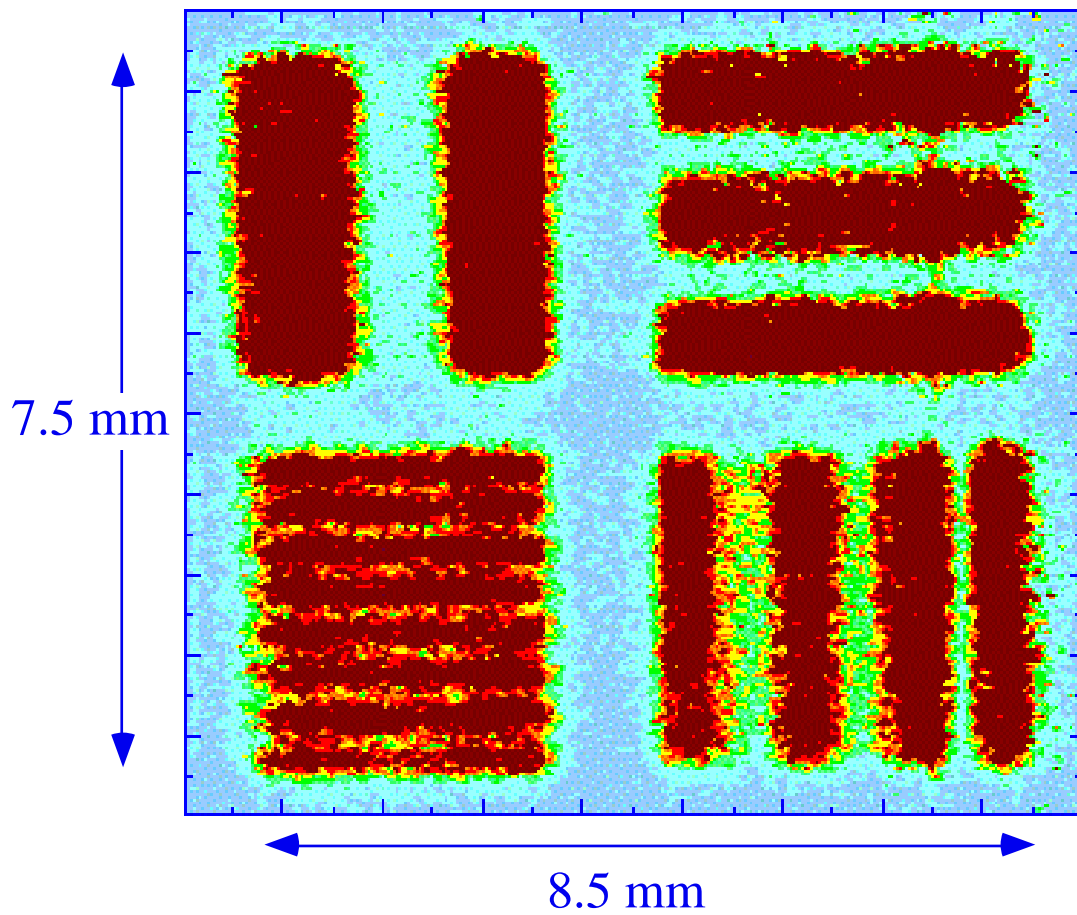


Fig. 8

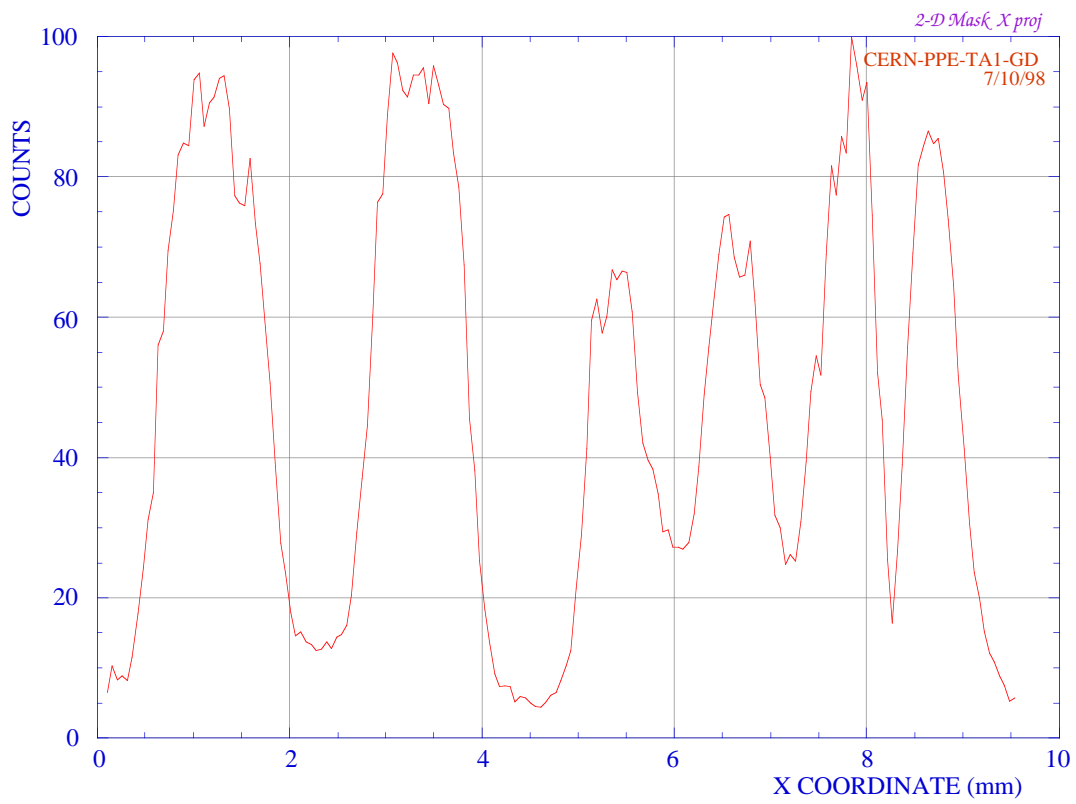
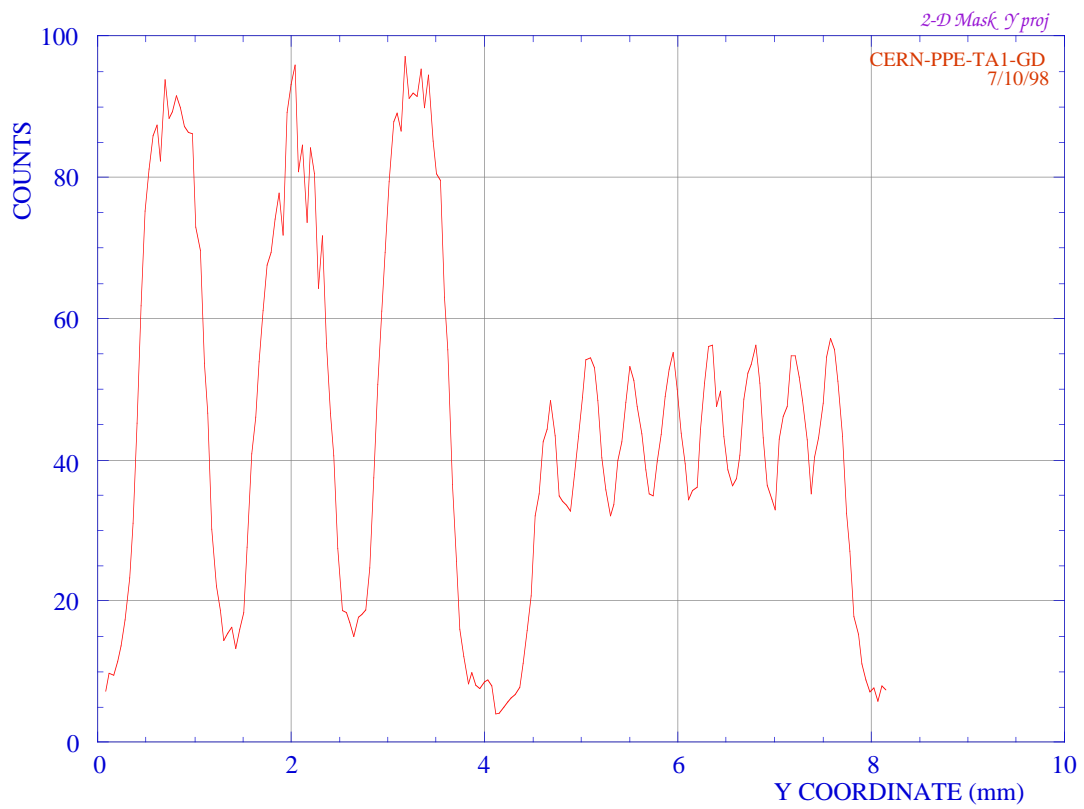
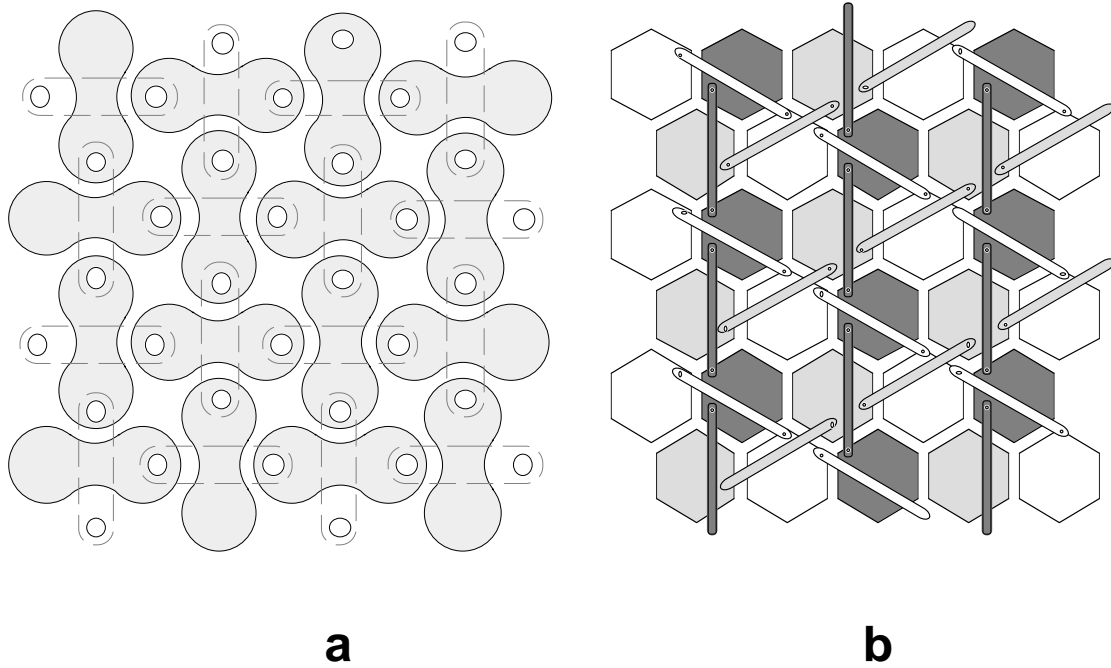


Fig. 9a



**Fig. 9b**



**Fig. 10**